Published in final edited form as:
J Phys Chem B. 2008 September 4; 112(35): 11147–11154. doi:10.1021/jp801175w.

Spermine Binding to Parkinson's Protein α-Synuclein and its Disease-Related A30P and A53T Mutants

Megan Grabenauer[†], **Summer L. Bernstein**[†], **Jennifer C. Lee**[‡,§], **Thomas Wyttenbach**[†], **Nicholas F. Dupuis**[†], **Harry B. Gray**[‡], **Jay R. Winkler**[‡], and **Michael T. Bowers**[†,*]

†*Department of Chemistry and Biochemistry, University of California, Santa Barbara, CA, 93106*

‡*Beckman Institute, California Institute of Technology, Pasadena, CA 91125*

Abstract

The aggregation of α-synuclein (α-syn), a protein implicated in Parkinson's disease (PD), is believed to progress through the formation of a partially folded intermediate. Using nano-electrospray ionization (ESI) mass spectrometry combined with ion mobility measurements we found evidence for a highly compact partially folded family of structures for α-syn and its disease-related A53T mutant with net charges of −6, −7 and −8. For the other early-onset PD mutant, A30P, this highly compact population was only evident when the protein had a net charge of −6. When bound to spermine near physiologic pH, all three proteins underwent a charge reduction from the favored solution charge state of −10 to a net charge of −6. This charge reduction is accompanied by a dramatic size reduction of about a factor of two (cross section of 2600Å^2 (−10 charge state) down to 1430Å^2 (−6 charge state)). We conclude that spermine increases the aggregation rate of α-syn by inducing a collapsed conformation, which then proceeds to form aggregates.

Keywords

alpha-synuclein; α-synuclein; aggregation; protein misfolding; Parkinson's Disease; ion mobility; spermine

Introduction

α-synuclein (α-syn) is the primary proteinaceous material implicated in the pathogenesis of Parkinson's disease (PD). Although the etiology of PD is still unknown, α-syn became the focus of PD research when it was first discovered as the primary fibrillar component in Lewy bodies and Lewy neurites found in the brains of PD patients.[1] Additionally, rare inherited autosomal early-onset forms of PD are linked to two missense mutations, A53T and A30P, found in the gene that codes for α-syn.[2,3] In recent years, a growing body of evidence suggests that oligomeric assemblies of α-syn are responsible for the toxic effects seen in PD and that the fibrillar deposits are perhaps a byproduct of neuronal death.[4–6]

α-syn belongs to a family of closely related presynaptic proteins. It is highly soluble and has 140 amino acid residues including seven imperfect repeats near the N-terminal region and a highly acidic C-terminal region. *In vitro* studies of α-syn and the A30P and A53T mutants

*Corresponding Author: Dr. Michael T. Bowers, Department of Chemistry and Biochemistry, University of California, Santa Barbara, CA 93106 Phone: (805) 893-2893 Fax: (805) 893-8703 Email: bowers@chem.ucsb.edu.
§Current Address: Laboratory of Molecular Biophysics, National Heart, Lung, and Blood Institute, National Institutes of Health, Bethesda, MD 20892

show the proteins are natively unfolded, having little or no ordered structure in the soluble form under physiological conditions.[7–9] Small-angle x-ray scattering studies indicate that at neutral pH these proteins have radii of gyration of about 40Å, larger than expected for a folded globular protein (15Å), and smaller than predicted for a random coil conformation (52Å).[7, 10] Fibrillization is believed to be a byproduct of α-syn misfolding that occurs in a nucleation dependent mechanism[4] initiated by a critical structural transformation from an unfolded conformation to a partially folded intermediate.[7] These studies indicate that α-syn most likely populates several intermediate conformations, both monomeric and oligomeric, on the pathway to the mature fibril form.[7,11] The rate of aggregation is affected by both the A53T and A30P mutations. It is generally agreed upon that the A53T mutation increases the rate of aggregation,[4,11–14] but studies on the A30P mutation have been far less conclusive. There are reports of faster aggregation,[13] of similar aggregation rates,[14] and of more rapid monomer consumption but slower fibril formation relative to WT α-syn.[4,11,12]

Spermine is a naturally occurring polyamine found in neuronal cells[15–17] that has, along with other polyamines, been shown to increase the rate of aggregation and fibrillation of α-syn.[18, 19] Although a complete profile of its functions is still unknown, spermine is known to be involved in neurodegenerative processes.[20] At physiological pH, spermine exists as a polycation and forms a complex with α-syn. This complex formation increases the rate of α-syn fibrillation without inducing significant secondary structure in this natively unfolded protein.[18,19,21] A recent NMR study demonstrated that although spermine is known to bind in the highly acidic C-terminal region, the complex ^{1}H-^{15}N HSQC spectrum shows significant intensity changes in the peaks corresponding to glycine and threonine residues in the N-terminal region, amino acids 22–93, as compared to the free protein.[21] The two mutants investigated in this study, A30P and A53T, have substitutions in this region and we were curious to see if these substitutions had a significant effect on the complex structures.

It is critical to pursue methods that give insight into the actual structure of the α-syn monomers and probe any structural transitions that may occur in order to develop effective therapeutic strategies. Ion mobility spectroscopy is a powerful method for achieving this goal, allowing accurate measurement of collision cross sections (shape). In this study we used ion mobility mass spectrometry to examine the structural features of the A30P and A53T mutant monomers and spermine complexes in comparison to WT α-syn.

Materials and Methods

Sample Preparation

Spermine was purchased from Sigma (St. Louis, Mo) and used without further purification. All α-syn samples were purchased from rPeptide (Bogart, Ga). Samples for nano-ESI experiments were prepared by dissolving the lyophilized proteins in water to make concentrated stock solutions. pH 7.5 and pH 2.5 solutions were prepared by dialyzing the stock solutions in 10mM ammonium acetate overnight using Slide-a-lyzer Mini Dialysis Units (3.5K MWCO, Pierce Biotechnology, Rockford, IL). Samples were then filtered using Microcon YM-100 Centrifugal Filter Devices (100K MWCO, Millipore Corp., Billerica, MA) to filter out large aggregates, and adjusted to the desired pH using NH_4OH and CH_3COOH. The concentrations were determined from UV absorption using an estimated extinction coefficient of 5120 $M^{-1}cm^{-1}$ at 280 nm.[22] Solutions were diluted to ~ 5–10 μM concentrations immediately prior to use. For samples containing spermine, spermine was added after this final dilution in a 1:10 α-syn to spermine ratio. Samples were left in a refrigerator overnight, to improve binding, before running.

Instrumentation

Details of the experimental set up for obtaining mass spectra and ion mobilities have previously been published elsewhere,[23] so only a brief description will be given here. The instrument consists of a nano electrospray ionization (nano-ESI) source, an ion funnel, a drift cell, and a quadrupole mass filter. Ions are generated in the source from ~ 5 μL of sample solution contained in a metal coated borosilicate capillary (Proxeon, Odense, Denmark). A continuous beam of ions is created and injected into the ion funnel. The ion funnel acts as an interface between the source and high vacuum chamber and transports the ions to the drift cell without the use of high acceleration fields. The drift cell is filled with ~ 5 torr of helium buffer gas and is followed by a quadrupole mass filter and a detector. To obtain mass spectra a continuous beam of ions passes through the drift cell and quadrupole mass filter before arriving at the detector.

To obtain mobility data the ion funnel is used as a storage device and the ions are pulsed into the drift cell triggering a timing sequence. Once the ions enter the cell, they are quickly thermalized by collisions with the helium buffer gas and are pulled through the drift cell by a weak electric field, E. Due to the counterbalance of the forward acceleration and the frictional drag, the ions obtain a constant drift velocity, v_D, proportional to E

$$v_D = K \cdot E \tag{1}$$

where the proportionality constant K is the ion mobility. In the low field limit, K is a function of the buffer gas pressure, P, the temperature, T, the reduced mass, μ, of the colliding particles (ion + He), and the ion's collision cross section, s.

Once the ions exit the drift cell, they pass through the quadrupole mass filter and are detected as a function of time, producing an arrival time distribution (ATD). Through the use of kinetic theory, the mobility is related to the collision-cross section, s, as given in equation 2:[24]

$$\sigma = 1.3\left(\frac{z^2 E^2 T}{\mu k_B P^2 N^2 l^2}\right)^{1/2}(t_A - t_0) \tag{2}$$

where z is the charge on the ion, k_B is the Boltzmann constant, N is the He number density at STP, l is the length of the cell, t_A is the time it takes the ion to arrive at the detector after the initial pulse into the drift cell, and t_0 is the time it takes the ions to reach the detector after exiting the drift cell. Since all of the constants in equation (2) are known for a given experiment and P, T, E, and t_A and t_0 can be very accurately measured, a precise value of σ is obtained.

The injection energy with which ions enter the drift cell is an important variable. At low injection energies the ions are gently pushed into the cell and only need a few "cooling" collisions to reach thermal equilibrium with the buffer gas. At high injection energies the larger collision energy leads to internal excitation of the ions before cooling and equilibrium occur. This can lead to isomerization to the most stable gas phase conformations or dissociation of dimers and higher-order oligomers if they are present. Unless otherwise stated, all mass spectra and ATDs were taken at an intermediate injection energy value of 40–50eV.

Results

Negative ion mass spectra were collected at pH 2.5 and pH 7.5 for WT α-syn and its A30P and A53T mutants. Negative ion mode was chosen due to the large number of acidic residues, D

and E, relative to basic residues, K and R in the amino acid sequence of the proteins (24 compared to 15) resulting in a net negative charge in solution at neutral pH. As all three proteins produced very similar mass spectra, only the A30P mutant spectra are presented in Fig. 1. The negative ion mass spectrum of the A30P mutant at pH 7.5 shows a broad distribution of charge states ranging from −6 to −17, centered at −13. There is also a second smaller distribution of half integer charge states (i.e. z/n = −15/2, −17/2… where z is the ion charge and n is the oligomer order). At pH 2.5 the charge state distribution is shifted to lower charge states, centered at −9, significantly narrowed, ranging only from −6 to −11, and the half integer charge states no longer appear. This shift in charge state distribution is consistent with a protein that is natively unfolded at pH 7.5 and partially folded at pH 2.5.[25–28] In addition, the smaller aggregates appear to have further aggregated to larger oligomers out of the mass range of our quadrupole. These same trends are observed for the A53T mutant as well as WT α-syn.[29]

Arrival Time Distributions (ATDs) were obtained, and cross sections measured, for charge states −6 and above for each sample. For charge states that were present at both pH 2.5 and pH 7.5, ATDs and cross sections are comparable at each pH, the one exception being the −10 charge state for the two mutants. The A30P mutant −10 ATD contains a single peak at pH 2.5 but has two features at pH 7.5 while the A53T mutant −10 ATD contains two features at pH 2.5 and only a single peak at pH 7.5. It is important to note however that the overall peak width and average cross section of this charge state for both mutants is the same at each pH. In addition, multiple features are present in the ATDs for the low charge states −6 through −8 for WT α-syn and the A53T mutant, and −6 through −9 for the A30P mutant.

The mass spectrum at pH 7.5 in Fig. 1 contains a charge state distribution composed of half integer charge states which arises from the presence of multiply charged oligomers. Therefore, a percentage of each monomer peak in the mass spectrum may be composed of multiply charged oligomer (a monomer with 7 charges and a dimer with 14 charges have the same z/n value) which may contribute to the ATD for that charge state. However, data was taken under a variety of solution conditions (data not shown) some of which led to mass spectra in which no evidence for multiply charged oligomers was present. In all cases, the overall ATD peak width for a particular whole number charge state and the structures in the ATD are conserved, i.e. the ATDs for the −6 charge state look essentially the same regardless of how much multiply charged oligomer is observable in the mass spectrum. Since the ATDs for samples where oligomers were present in the mass spectrum appear qualitatively the same as ATDs for samples with no multiply charged oligomers present in the mass spectrum, it appears that we are primarily observing the ATDs for monomeric forms of the protein for whole integer z/n peaks. The ATDs presented in Fig. 2 and Fig 3 were taken at pH 2.5 where no dimer peaks are observed under any source conditions so these are unambiguously pure monomer ATDs.

For each of the ATDs exhibiting multiple features, the dominant feature varies with injection energy, as shown in Fig. 2 for the WT α-syn −7 ATD at pH 2.5. At low injection energy (30 eV), the ATD has a broad distribution centered near 870 μs. The broadness of the distribution implies that there are several conformers present, and a dominant family of structures with an average cross section of 1730 $Å^2$. When the injection energy is increased (50 eV), the ATD is shifted toward later arrival times. At high injection energy (100 eV), a dominant family of structures is seen again, this time with an average cross section of 2078 $Å^2$. These results suggest the more compact structures are present in solution, and we observe these at low injection energies, but as the injection energy is increased they are annealed to a family of more extended structures preferred in the solvent-free state.

At higher charge states the ATDs all become much narrower and contain a single feature. Fig. 3 shows a comparison of ATDs taken at pH 2.5 for several charge states of WT α-syn and both the A30P and A53T mutants. ATDs for WT α-syn and the A53T mutant at each charge state

are very similar. For the −7 and −8 charge states, ATDs for WT α-syn and the A53T mutant are much broader than the corresponding ATDs for the A30P mutant. For these charge states the A30P mutant populates more extended families of structures than WT α-syn and the A53T mutant. ATDs for the −9 charge state for each protein have similar widths, although the A30P mutant ATD has multiple features. However, the broadness of the WT α-syn and A53T mutant ATDs could easily contain multiple unresolved features. After the −9 charge state, all three proteins have significantly narrowed distributions and for charge states −11 and above they all contain a single well defined peak as exemplified by the −12 charge state.

Cross sections measured for the monomer charge states of all three samples are summarized in Fig. 4. Since pH does not appear to affect the cross sections, average cross sections across both pHs are plotted. There is a family of relatively compact structures dominant in low charge states and one of more extended structures dominant in high charge states. For WT α-syn and the A53T mutant the compact family of structures is present in charge states −6 through −8. For the A30P mutant however, this compact family is seen only in the −6 charge state. The extended family of structures in all three proteins increases in cross section with charge state due to Coulomb repulsion between the charges leading to more open structures and larger cross sections as *z/n* increases.

When spermine was added to the protein solutions a stable spray could not be obtained from acidic solutions, but good data were obtained for neutral solutions. A mass spectrum of the pure A53T mutant is given in Fig. 5a for reference. As shown in Fig. 5b, at an intermediate injection energy of 50ev, when spermine is added a bimodal distribution of charge states is observed with −9 being locally dominant, but −6 clearly being the dominant charge state overall. This represents a huge shift in the dominant charge state, which ranges from −11 through −13 for the neutral solutions without spermine, where the −6 peak is barely visible. Satellite peaks are clearly visible at higher mass representing α-syn/spermine complexes and the dimer peaks evident at half integral *z/n* values in Fig. 5a have disappeared, most likely due to increased oligomerization. One very interesting thing about this spectrum is that not only is the $[\alpha\text{-syn} + \text{spermine}]^{-6}$ peak the largest of the complex peaks, but $[\alpha\text{-syn}]^{-6}$ is the largest unbound charge state as well. At a high injection energy of 100ev, Fig. 5c, the α-syn/spermine complex peaks are no longer observed, and large unresolved peaks from dissociation of higher order oligomers are present. In addition, highly charged monomers are observed that are only weakly present in Fig. 5b, presumably from monomer dissociation from the large oligomers.[30,31]

ATDs for the −6 charge state of the A53T mutant from solutions both with and without spermine at an injection energy of 50eV are given in Fig. 6. All three ATDs are complex with families of conformations having cross sections near 1440$Å^2$ and 1780 $Å^2$. The relative intensities of the peaks in the ATDs of the free protein in solution and the unbound protein in the complex solution are very similar, while the peak corresponding to the more compact conformational family dominates the ATD of the α-syn/spermine complex. Of interest is the fact that no new conformational families were observed, only a strong shift to more compact structures. WT α-syn and the A30P mutant gave similar results. It is also important to notice that no dimers are present in the mass spectrum in Fig. 5b that yielded the ATDs in Fig. 6b and Fig. 6c. Hence, these ATDs are due to pure monomer. The ATD in Fig 6a is very similar to the one in Fig. 6b, strongly supporting the fact it is also due to monomer.

Discussion

As shown in Fig. 1 the A30P mutant has a much narrower and lower charge state distribution at pH 2.5 than at pH 7.5. This same behavior is observed for the A53T mutant and WT α-syn,[29] as well. The shift in charge state distribution alone is evidence that the protein is more

compact under acidic compared to physiologic conditions,[25–28] but further evidence comes from looking beyond charge state distribution and comparing the cross sections of each charge state. Since low charge states have smaller cross sections, and more of the protein exists in low charge states at pH 2.5 than at pH 7.5, this implies that the protein is more compact at the lower pH. A number of factors are known to trigger aggregation in WT α-syn by inducing a partially folded state, including low pH.[7]

ATDs for WT α-syn and the A53T mutant show evidence of a highly compact, partially folded family of structures for net charges −6, −7 and −8. The A30P mutant ATDs however only demonstrate this partially folded state at a net charge of −6. As can be seen in Fig. 4 the cross sections of the more extended families of structures for the −7 and −8 charge states are very similar for all three proteins, but the smallest structures observed for the A30P mutant are 30–40% larger than the smallest structures observed for WT α-syn and the A53T mutant. Fluorescence energy-transfer (FET) kinetics experiments by Lee *et al*[32] have shown that the distances between two donor/acceptor pairs in the vicinity of residue 30 were increased for the A30P mutant relative to WT α-syn in neutral solutions, while in acidic solutions the distances decreased. Since our results show an increase in cross section at both neutral and acidic pHs, the mutation must be inducing a large scale structural change in the protein that outweighs this localized compaction in acidic conditions. The single residue mutation, substitution of a proline in place of an alanine, causes a significant increase in the overall size of the compact structures of α-syn and most likely prevents the formation of the partially folded intermediate with a net charge of more than −6. This dramatic dependence of foldedness on charge may account for some of the inconclusive results on aggregation rates of the A30P mutant compared to WT α-syn.[4,11–14] The A30P mutation is known to disrupt a region of residual helical structure found near the N-terminus in the WT protein,[33] and this may be a contributing factor for the increase in cross sections that we observe.

Another factor known to increase α-syn aggregation is binding with cationic species such as metal ions[34–38] and polyamines.[18,19,21] Interestingly, while metal ion binding is thought to increase aggregation by facilitating collapse into a partially folded state,[37] binding of polyamines appears to trigger aggregation without inducing significant changes in secondary structure.[18,19,21] One of the most effective polyamines in this respect is spermine, a naturally occurring polyamine that binds to α-syn via a specific interaction with the C-terminus and increases the kinetic efficiency of aggregation by 10^5.[21] Recent NMR studies have shown that although spermine binds near the C-terminus, structural changes may occur near the N-terminus, particularly affecting glycine and threonine residues in the region aa22–93.[21,39] In spite of this interaction, data collected for the A53T mutant, which introduces a threonine residue in the aa22–93 region, were the same as that for WT α-syn and the A30P mutant.

Addition of spermine to all three protein samples results in a dominant charge state of −6 in each mass spectrum. In solution at pH 7.5, the protein exists in an equilibrium of conformations, but being natively unfolded at this pH, the majority of α-syn is expected to have a net charge between −9 and −10. A plot of net charge on α-syn vs. pH, as estimated from the protein sequence and amino acid pKa values[40], is given in Fig. 7. At pH 7.5 spermine, shown schematically in Fig. 5b, exists as a polycation with net charge +4 so it is reasonable to predict that in solution the net charge of the protein/cation complex is −6. The dominance of the −6 charge state in the mass spectrum of the α-syn/spermine mixture (Fig. 5b) and the presence of a bimodal charge state distribution, rather than a shift of the original charge state distribution by four charges, shows that spermine forms a compact folded complex with α-syn in solution, reducing the number of sites available for deprotonation during electrospray. Looking at the ATDs for this charge state, we do not see any new conformational families but we do see a significant shift in intensity to favor the more compact structures in the complex as compared to the unbound protein. However, it is important to recall that spermine is binding to a protein

with a net charge of −10 in solution (average cross section near 2600Å^2), reducing the charge to −6 and reducing the cross section of most of the protein to 1430Å^2, a size reduction of nearly a factor of two. Some very small fraction of uncomplexed α-syn exists in the −6 charge state in pure α-syn solutions under physiological conditions and a fraction of that small fraction is in the compact conformation. However, when spermine is added α-syn/spermine complexation results, yielding nearly 100% compact α-syn.

The fact that not only is the −6 charge state dominant in the α-syn/spermine complex charge state distribution but also in the free α-syn protein distribution strongly suggests that in solution an [α-syn + spermine]$^{-6}$ complex is dominantly formed, which then partially dissociates to form [α-syn]$^{-6}$ and neutral spermine upon being sprayed, dehydrated, and traversing the IMS-MS instrument. Since the [α-syn]$^{-6}$ ATD in the α-syn/spermine mixture closely resembles the ATD from the pure α-syn sample, some refolding/unfolding must occur upon spermine dissociation. The 1430Å^2 structure is most likely a “solution” structure, while the 1780 Å^2 structure is a “solvent-free” structure which results from unfolding once spermine dissociates. This process is shown schematically in Fig. 8. (This interpretation is also consistent with the 1730Å$_2$ structure for [α-syn]$^{-7}$ unfolding to a “solvent-free” structure at 2078Å^2 as injection energy is increased (Fig. 2)). Exactly where the dissociation of the α-syn/spermine complex occurs is not apparent, but the lower intensity of the complex peak compared to the unbound protein peak implies that it does occur somewhere, since it has previously been shown[41] that a significant amount of spermine bound protein can be detected by ESI-MS. Our instrumentation[23] is very different from most commercial mass spectrometers in that it incorporates an ion funnel to capture, desolvate, and transport the ions coming out of the capillary, and a drift cell filled with ~5 torr of helium buffer gas. A significant amount of energy must be imparted to the ions in order to inject them from vacuum into the drift cell, and this step may account for dissociation of the complex. In fact, as injection energy is increased, the α-syn/spermine complex is essentially completely dissociated (see Fig. 5c).

It has been shown that the rate of fibrillization of α-syn *in vitro* is significantly increased by the presence of certain metal ions[34–38] most likely due to the metals’ ability to mask electrostatic repulsions and facilitate collapse into a partially folded intermediate.[7,42] We propose that a similar process, illustrated in Fig. 9, takes place upon the addition of spermine. In the protein solution without spermine, a range of conformations exists in equilibrium, a small fraction of which are compact while the majority are extended. Once spermine is added, most of the extended conformations are rearranged to become more compact due to the dramatic charge reduction. This α-syn/spermine complex doesn’t appear to result in any new structures as the cross sections are very similar to the compact form of the free −6 α-syn protein. We hypothesize that it is these more compact conformations that aggregate and go on to form fibrils. In the solution with no spermine, there are very few of these compact conformations so aggregation will proceed slowly. In the presence of spermine however, the higher proportion of compact conformations induces faster aggregation possibly accounting for the 10^5 increase in aggregation efficiency.[21]

The mechanism of α-syn aggregation in the presence of spermine is still not well understood and models of the process are varied. Electron capture dissociation[41] (ECD), and NMR[39] studies have proposed that spermine binding to α-syn leads to larger, more extended structures. It has been suggested that charge shielding resulting from spermine binding to the protein reduces intramolecular electrostatic interactions between the C-terminal region and central/N-terminal regions of α-syn, reducing the protein’s overall compactness and forming an open structure more favorable for self-assembly. It has also been proposed[19,43] that the increased rate of α-syn aggregation in the presence of spermine can be accounted for by the binding of spermine causing a reduction in electrostatic repulsion between molecules undergoing self-assembly. Alternatively, it has been suggested that the multivalent polyamine may act as a

bridge between protein monomers.[18,43] Like most natively unfolded proteins, WT α-syn and its A30P and A53T mutants are characterized by low hydrophobicity and high net charge.[44] Several independent studies have shown that the aggregation of amyloidogenic proteins/peptides is very much dependent on net charge, with a lower net charge leading to faster aggregation.[45–47] Reduction in net charge leading to a partially folded intermediate has been proposed as the mechanism by which cationic metal binding[7,42] and low pH[7] increase α-syn aggregation. In light of the dramatic compaction spermine induces in α-syn as shown here, it is reasonable to propose a similar effect from polyamines.

It is highly likely that protein aggregation is occurring in our experiments, as evidenced by the significant overall loss of signal in the α-syn/spermine solutions relative to the pure α-syn solutions (see enhanced noise level in Fig. 5b and Fig. 5c relative to Fig. 5a). Dimer peaks evident in spectra from the pure α-syn solutions (Fig. 5a) are not present in spectra from α-syn/spermine solutions (Fig. 5b), presumably because they have gone on to form higher order oligomers that are out of the mass range of our instrument. Increasing the injection energy causes some of the higher order oligomers to dissociate, creating observable oligomers within our mass range. These oligomers appear as large unresolved peaks in the mass spectrum shown in Fig. 5c.

It is important to consider how the solvent-free results presented here relate to solution structures. As Loo[48] has pointed out, there are several noncovalently bound protein ligand complexes in which the observed gas phase stoichiometry is in agreement with that expected in the solution. There have also been numerous studies in which elements of solution phase structure are preserved in the gas phase. Relevant examples include, but are not limited to, large protein assemblies such as GroEL-substrate complexes[49] and the 11-member ring complex formed by the *trp* RNA binding attenuation protein (TRAP),[50] globular monomeric proteins including cytochrome c,[51] and smaller biomolecules such as the Alzheimer's peptide amyloid-beta.[52] Our injection energy results indicate that at low injection energies compact structures are observed while at higher injection energies these tend to unfold, presumably to more favorable solvent-free structures. Hence, we are confident that the current results reflect solution properties of the system.

Conclusions

- Highly compact families of structures are present for WT α-syn and its A53T mutant with net charges of −6, −7 and −8. The A30P mutant only exists in a highly compact form with net charge −6, possibly accounting for its inconsistent aggregation behavior.
- All three proteins behave the same in the presence of spermine.
- Spermine effectively binds to an extended conformation and rearranges it to a much more compact form by lowering the net charge from −10 to −6.
- Mass spectral results suggest spermine complexation may induce oligomerization of α-syn.

Abbreviations

α-syn, α-synuclein; PD, Parkinson's Disease; ATD, Arrival Time Distribution; WT, Wild Type.

Acknowledgements

We thank Professor Joe Loo for suggesting the experiments with spermine and Dr. Catherine J. Carpenter for help with the preparation of figures. Support from National Science Foundation grant CHE-0503728 (MTB), National Institutes of Health grant GM068461 (JRW), the Ellison Medical Foundation (Senior Scholar Award in Aging to HBG), and the Arnold and Mabel Beckman Foundation (JCL) are gratefully acknowledged.

References

1. Dunnet SB, Bjorklund A. Nature 1999;399:A32–A39. [PubMed: 10392578]
2. Krüger R, Kuhn W, Müller T, Woitalla D, Graeber M, Kösel S, Przuntek H, Epplen JT, Schols L, Reiss O. Nat. Genet 1998;18:106–108. [PubMed: 9462735]
3. Polymeropoulos MH, Lavedan C, Leroy E, Ide SE, Dehejia A, Dutra A, Pike B, Root H, Rubenstein J, Boyer R, Stenroos ES, Chandrasekharappa S, Athanassiadou A, Papapetropoulos T, Johnson WG, Lazzarini AM, Duvoisin RC, DiIorio G, Golbe LI, Nussbaum RL. Science 1997;276:2045–2047. [PubMed: 9197268]
4. Conway KA, Lee SJ, Rochet JC, Ding TT, Williamson RE, Lansbury PT Jr. Proc. Natl. Acad. Sci. U. S. A 2000;97:571–576. [PubMed: 10639120]
5. Ding TT, Lee SJ, Rochet JC, Lansbury PTJ. Biochemistry 2002;41:10209–10217. [PubMed: 12162735]
6. Lansbury PT. Proc. Natl. Acad. Sci. U. S. A 1999;96:3342–3344. [PubMed: 10097040]
7. Uversky VN, Li J, Fink AL. J. Biol. Chem 2001;276:10737–10744. [PubMed: 11152691]
8. Weinreb PH, Zhen WG, Poon AW, Conway KA, Lansbury PT Jr. Biochemistry 1996;35:13709–13715. [PubMed: 8901511]
9. Dedmon MM, Lindorff-Larsen K, Christodoulou J, Vendruscolo M, Dobson CM. J. Am. Chem. Soc 2005;127:476–477. [PubMed: 15643843]
10. Li J, Uversky V, Fink AL. NeuroToxicology 2002;23:553–567. [PubMed: 12428728]
11. Conway KA, Harper JD, Lansbury PT. Nat. Med 1998;4:1318–1320. [PubMed: 9809558]
12. Li J, Uversky VN, Fink AL. Biochemistry 2001;40:11604–11613. [PubMed: 11560511]
13. Narhi L, Wood SJ, Steavenson S, Jiang Y, Wu GM, Anafi D, Kaufman SA, Martin F, Sitney K, Denis P, Louis J-C, Wypych J, Biere AL, Citron M. J. Biol. Chem 1999;274:9843–9846. [PubMed: 10092675]
14. Serpell LC, Berriman J, Jakes R, Goedert M, Crowther RA. Proc. Natl. Acad. Sci. U. S. A 2000;97:4897–4902. [PubMed: 10781096]
15. Gilad GM, Gilad VH. Int. J. Dev. Neurosci 1986;4:195–208. [PubMed: 3138895]
16. Slotkin TA, Bartolome J. Brain Res. Bull 1986;17:307–320. [PubMed: 3094839]
17. Vivo M, de Vera N, Cortes R, Mengod G, Camon L, Martinez E. Neurosci. Lett 2001;304:107–111. [PubMed: 11335066]
18. Antony T, Hoyer W, Cherny D, Heim G, Jovin TM, Subramaniam V. J. Biol. Chem 2003;278:3235–3240. [PubMed: 12435752]
19. Goers J, Uversky VN, Fink AL. Protein Sci 2003;12:702–707. [PubMed: 12649428]
20. Morrison LD, Cao XC, Kish SJ. J. Neurochem 1998;71:288–294. [PubMed: 9648877]
21. Fernandez CO, Hoyer W, Zweckstetter M, Jares-Erijman EA, Subramaniam V, Griesinger C, Jovin TM. EMBO J 2004;23:2039–2046. [PubMed: 15103328]
22. Gill SC, von Hippel PH. Anal. Biochem 1989;182:319–326. [PubMed: 2610349]
23. Wyttenbach T, Kemper PR, Bowers MT. Int. J. Mass Spectrom 2001;212:13–23.
24. Mason, EA.; McDaniel, EW. Transport Properties of Ions in Gases. New York: Wiley; 1978.
25. Fenn JB, Mann M, Meng CK, Wong SFW, Whitehouse CM. Mass Spectrom. Rev 1990;9:37–70.
26. Svoboda M, Meister W, Kitas EA, Vetter W. J. Mass Spectrom 1997;32:1117–1123. [PubMed: 9358632]
27. Chowdhury SK, V K, BT C. J. Am. Chem. Soc 1990;112:9012–9013.
28. Jarrold MF. Annu. Rev. Phys. Chem 2000;51:179–207. [PubMed: 11031280]

29. Bernstein SL, Liu DF, Wyttenbach T, Bowers MT, Lee JC, Gray HB, Winkler JR. J. Am. Soc. Mass Spectrom 2004;15:1435–1443. [PubMed: 15465356]
30. Jurchen JC, Garcia DE, Williams ER. J. Am. Soc. Mass Spectrom 2004;15:1408–1415. [PubMed: 15465353]
31. Bernstein SL, Dupuis NF, Lazo ND, Wyttenbach T, Condron MM, Bitan G, Teplow DB, Shea J-E, Ruotolo BT, Robinson CV, Bowers MT. Submitted for publication.
32. Lee JC, Langen R, Hummel P, Gray H, Winkler J. Proc. Natl. Acad. Sci. U. S. A 2004;101:16466–16471. [PubMed: 15536128]
33. Bussell R, Eliezer D. J. Biol. Chem 2001;276:45996–46003. [PubMed: 11590151]
34. Binolfi A, Rasia RM, Bertoncini CW, Ceolin M, Zweckstetter M, Griesinger C, Jovin TM, Fernandez CO. J. Am. Chem. Soc 2006;128:9893–9901. [PubMed: 16866548]JA0618649
35. Paik SR, Shin HJ, Lee JH, Chang CS, Kim J. Biochem. J 1999;340:821–828. [PubMed: 10359669]
36. Uversky VN, Li J, Bower K, Fink AL. NeuroToxicology 2002;23:527–536. [PubMed: 12428725]
37. Uversky VN, Li J, Fink AL. J. Biol. Chem 2001;276:44284–44296. [PubMed: 11553618]
38. Rasia RM, Bertoncini CW, Marsh D, Hoyer W, Cherny D, Zweckstetter M, Griesinger C, Jovin TM, Fernandez CO. Proc. Natl. Acad. Sci. U. S. A 2005;102:4294–4299. [PubMed: 15767574]
39. Bertoncini CW, Jung YS, Fernandez CO, Hoyer W, Griesinger C, Jovin TM, Zweckstetter M. Proc. Natl. Acad. Sci. U. S. A 2005;102:1430–1435. [PubMed: 15671169]
40. Lehninger, AL. Principles of Biochemistry. New York: Worth; 1982.
41. Xie YM, Zhang J, Yin S, Loo JA. J. Am. Chem. Soc 2006;128:14432–14433. [PubMed: 17090006]
42. Fink AL. Acc. Chem. Res 2006;39:628–634. [PubMed: 16981679]
43. Hoyer W, Cherny D, Subramaniam V, Jovin TM. Biochemistry 2004;43:16233–16242. [PubMed: 15610017]
44. Uversky VN, Gillespie JR, Fink AL. Proteins: Structure, Function, and Genetics 2000;41:415–427.
45. Chiti F, Calamai M, Taddei N, Stefani M, Ramponi G, Dobson CM. Proc. Natl. Acad. Sci. U. S. A 2002;99:16419–16426. [PubMed: 12374855]
46. Schmittschmitt JP, Scholtz JM. Protein Sci 2003;12:2374–2378. [PubMed: 14500896]
47. Guo M, Gorman PM, Rico M, Chakrabartty A, Laurents DV. FEBS Lett 2005;579:3574–3578. [PubMed: 15964569]
48. Loo JA. Int. J. Mass Spectrom 2000;200:175–186.
49. van Duijn E, Simmons DA, van den Heuvel RHH, Bakkes PJ, van Heerikhuizen H, Heeren RMA, Robinson CV, van der Vies SM, Heck AJR. J. Am. Chem. Soc 2006;128:4694–4702. [PubMed: 16594706]
50. Ruotolo BT, Giles K, Campuzano I, Sandercock AM, Bateman RH, Robinson CV. Science 2005;310:1658–1661. [PubMed: 16293722]
51. Valentine SJ, Clemmer DE. J. Am. Chem. Soc 1997;119:3558–3566.
52. Baumketner A, Bernstein SL, Wyttenbach T, Bitan G, Teplow DB, Bowers MT, Shea J-E. Protein Sci 2006;15:420–428. [PubMed: 16501222]

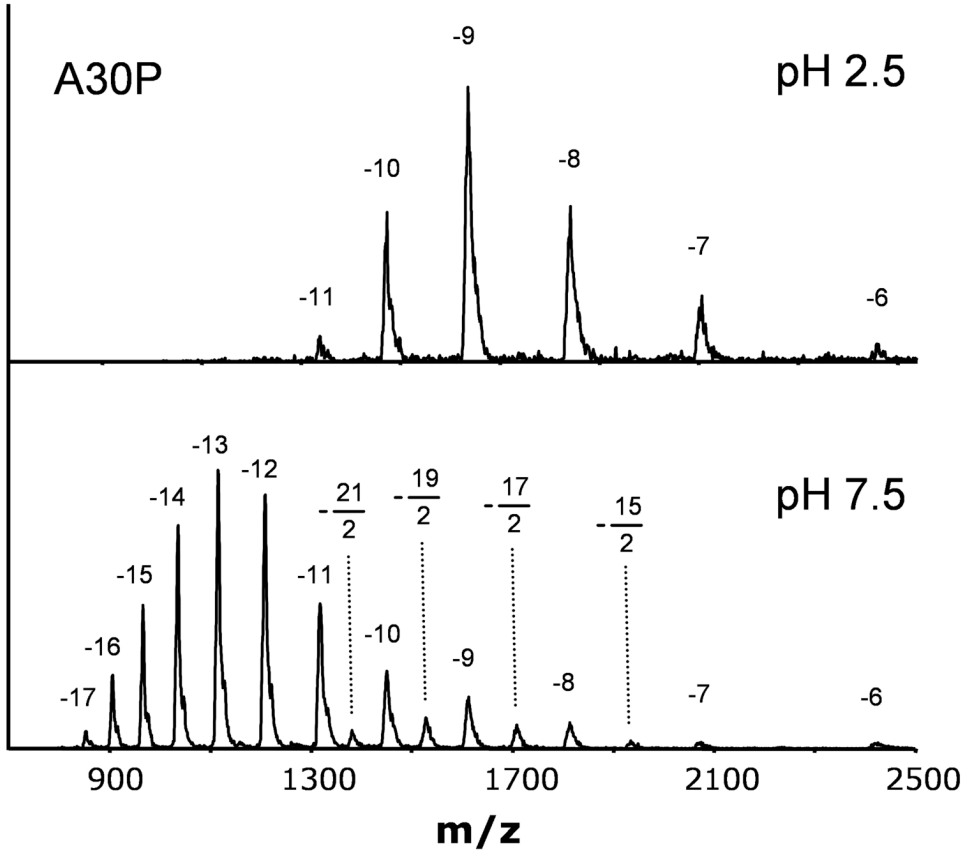

Fig. 1.

The negative ion mass spectrum of A30P α-syn shows a broad distribution at pH 7.5 which is shifted to lower charge states and significantly narrowed at pH 2.5.

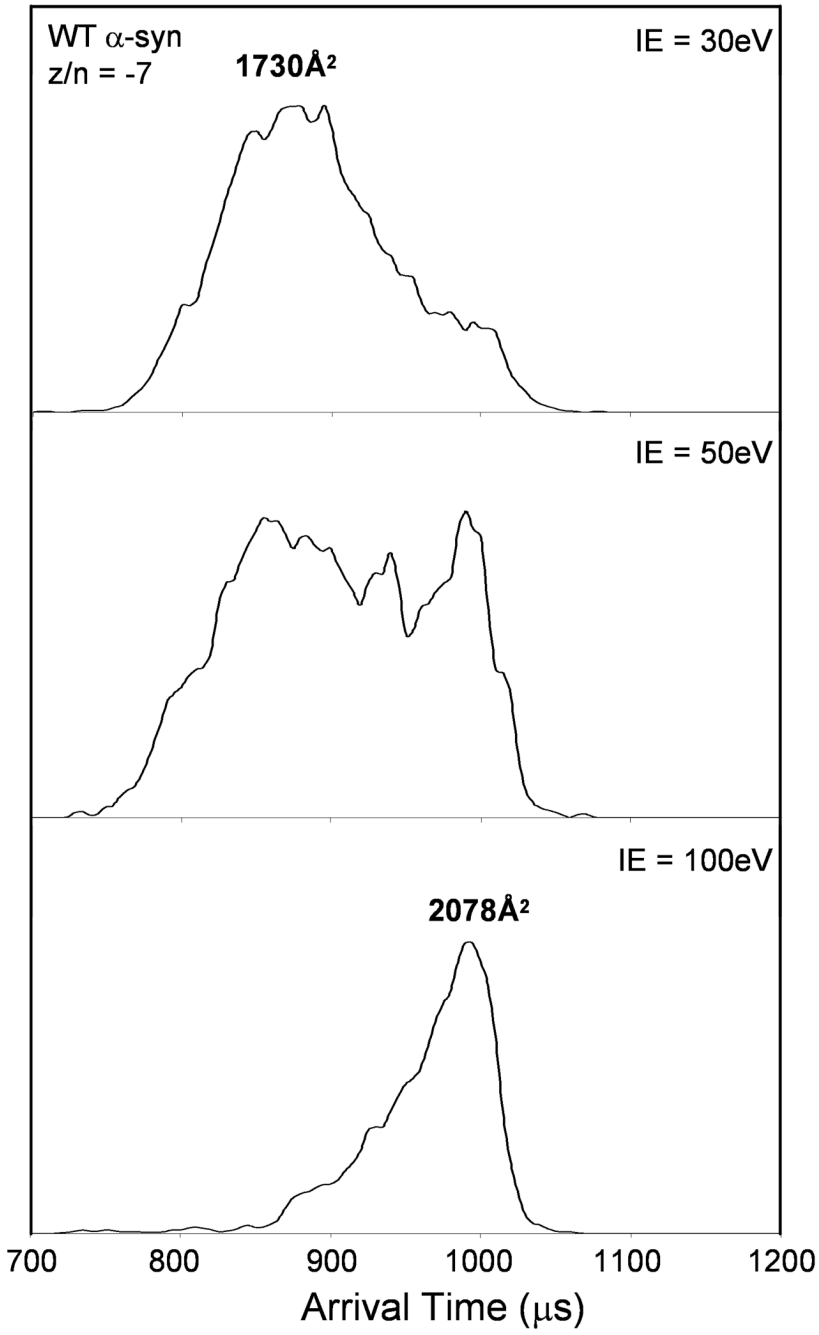

Fig. 2.
The ATD for the −7 charge state of WT α-syn at pH 2.5 demonstrates how the dominant features of low charge state ATDs vary with injection energy.

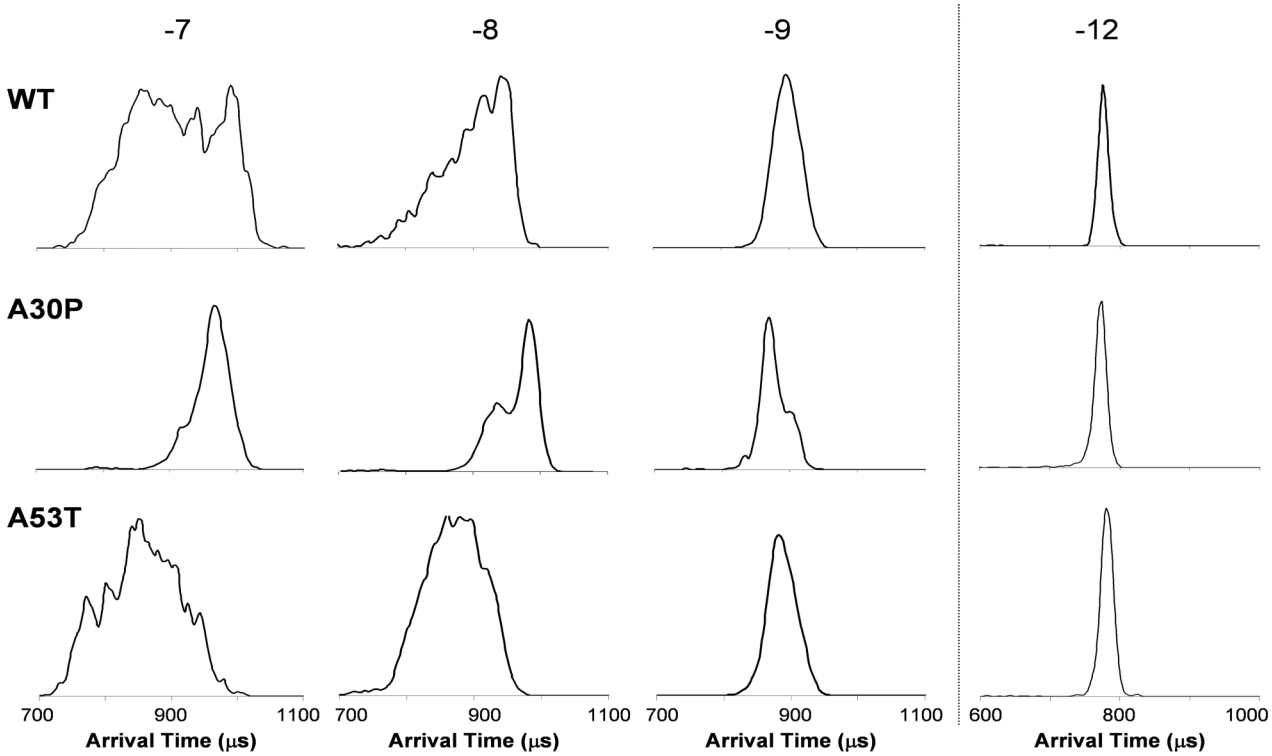

Fig. 3.

ATDs of several charge states taken at an injection energy of 50eV at pH 2.5. For charge states −7 and −8 the A30P mutant ATDs are much narrower than the WT and A53T mutant ATDs.

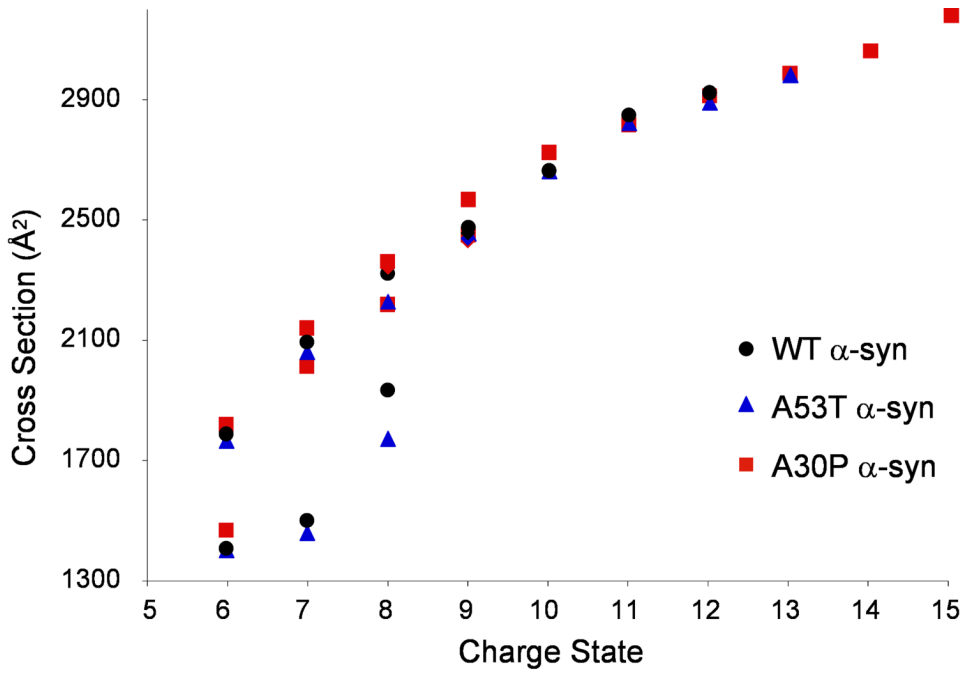

Fig. 4.

Cross section vs. charge state for WT α-syn and its A53T and A30P mutants. Two families of structures are clearly evident, one dominant in low charge states and one dominant in high charge states.

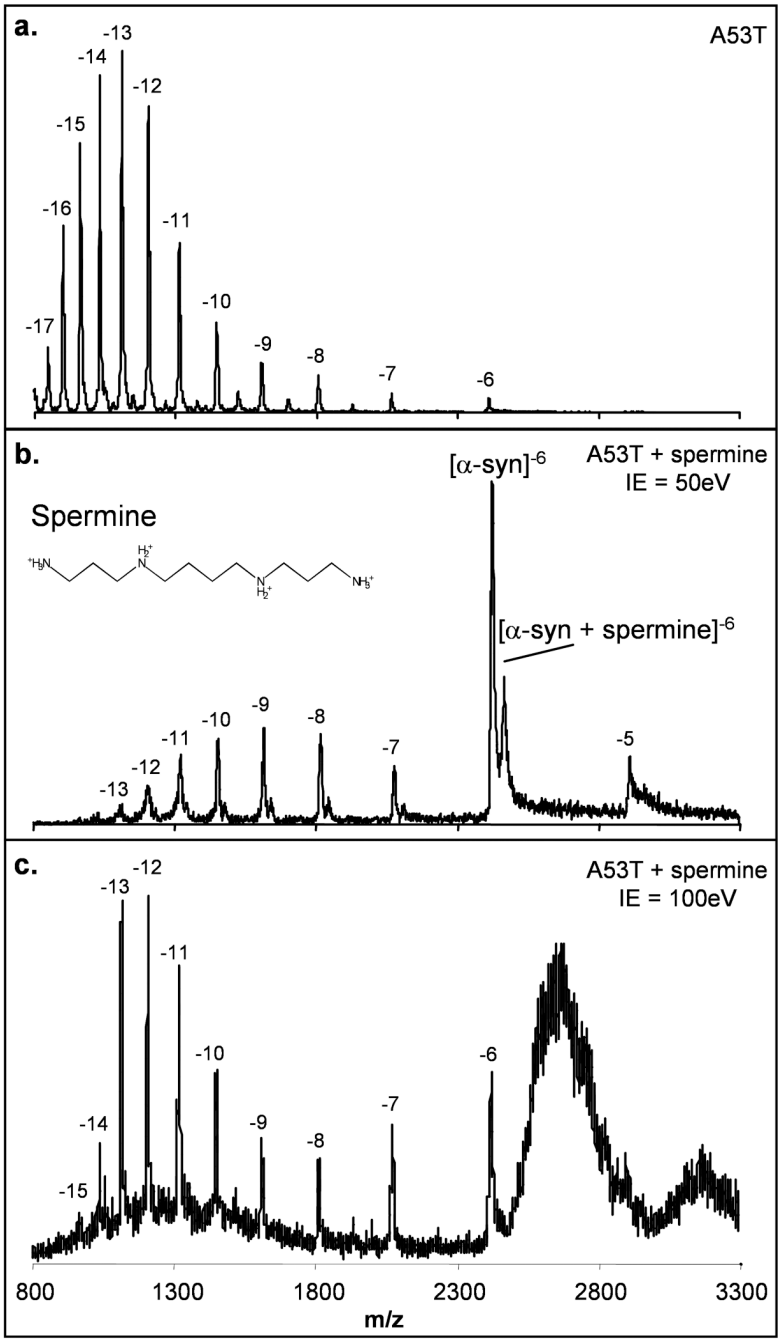

Fig. 5.

Negative ion mass spectrum of pure A53T α-syn taken at pH 7.5 with an intermediate injection energy of 50eV (a). Upon addition of spermine under the same conditions (b) the charge state distribution is dramatically shifted and α-syn/spermine complex peaks are observed. At a high injection energy of 100eV (c), the complex peaks are no longer easily observed, and large unresolved peaks from dissociation of higher order oligomers are present.

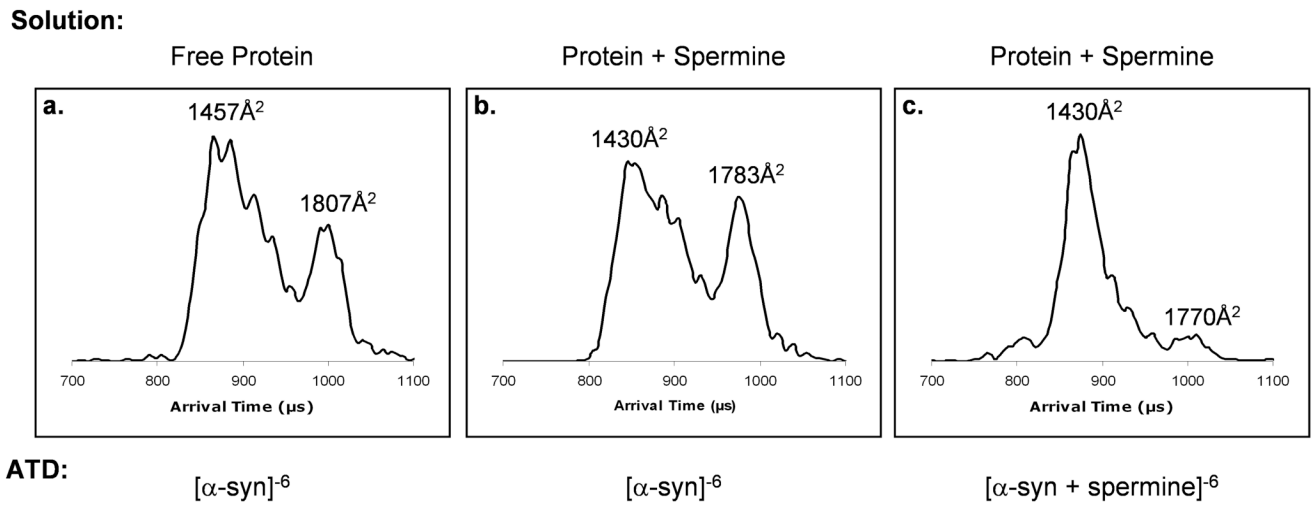

Fig. 6.

ATDs of the A53T α-syn mutant showing the presence of similar conformational families in the free protein in solution (a), the unbound protein in the complex solution (b), and the protein-spermine complex (c). A significantly greater percentage of the population is in the compact form in the complex as compared to the unbound protein.

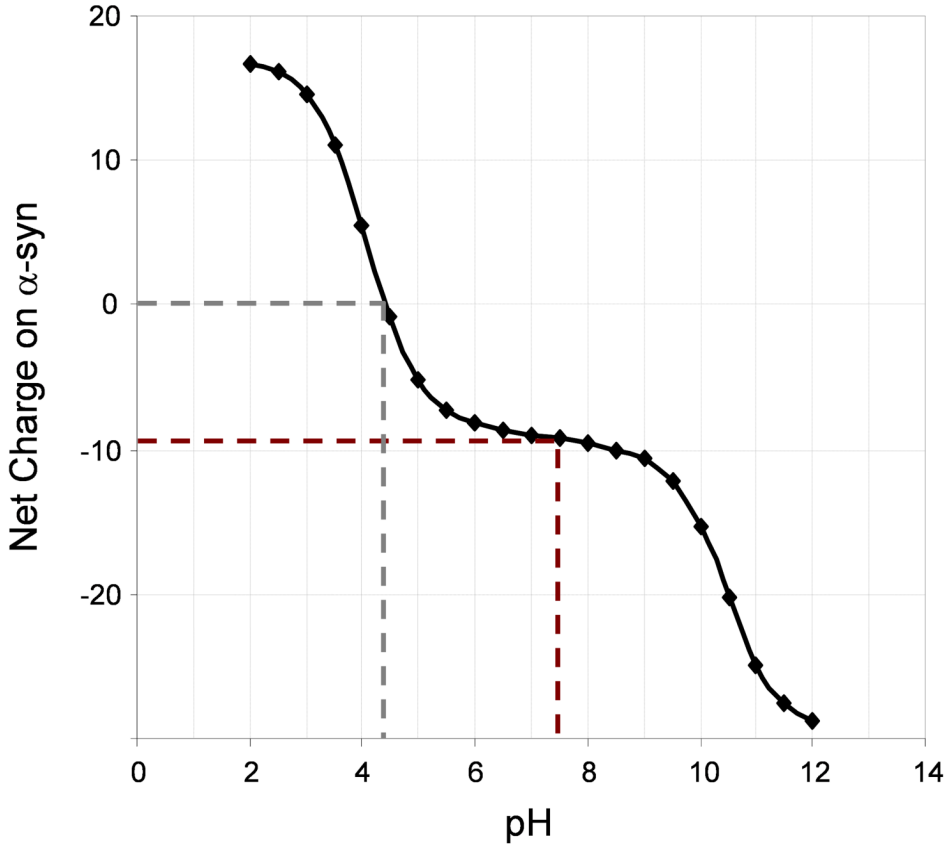

Fig. 7.
Plot of net charge on α-syn vs. pH, as estimated from its amino acid composition.

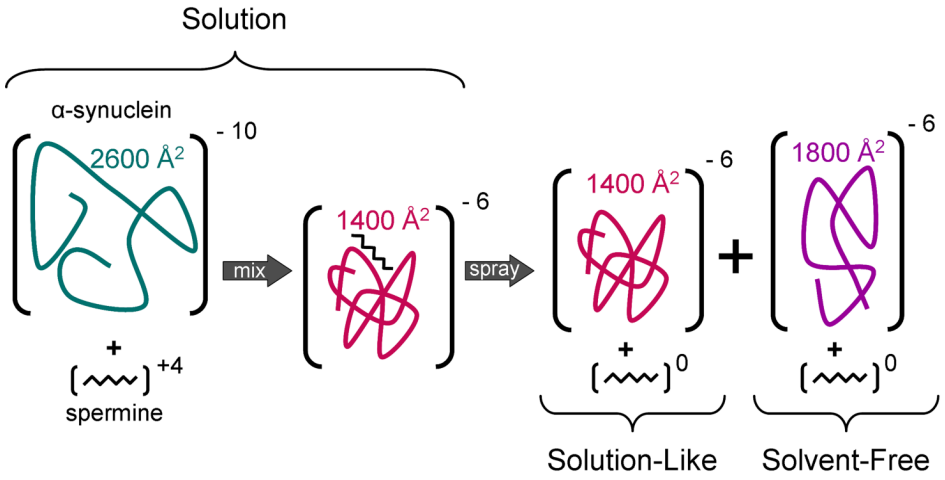

Fig. 8.
Schematic representation of spermine binding to α-syn, rearranging the protein, then dissociating as a neutral molecule.

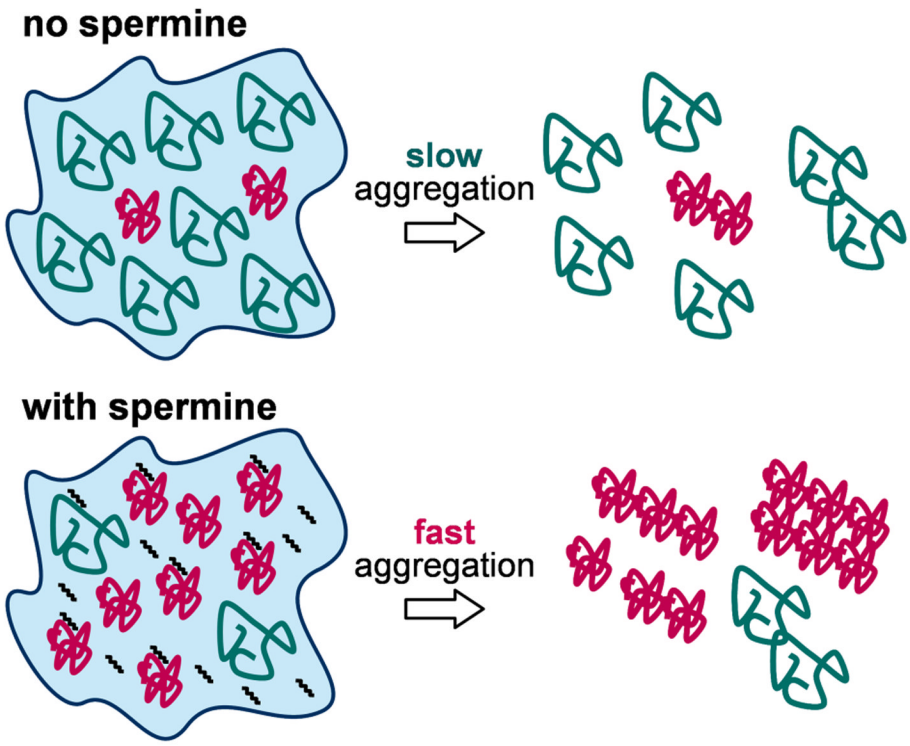

Fig. 9.
Illustration of a hypothetical mechanism for the accelerated aggregation of α-syn due to spermine binding.